CO_2-mineralization and carbonation reactor rig: design and validation for *in situ* neutron scattering experiments - Engineering and Lessons Learned

Ali Mortazavi,[a] Fu Song,[b] Michael Dudman,[a] Michael Evans,[c] Robert Copcutt,[c] Giovanni Romanelli,[d] Franz Demmel,[a] David H. Farrar,[e] Stewart F. Parker,[a] Kun V. Tian 田坤,[e,f,g,*] Devis Di Tommaso[b,*] and Gregory A. Chass[b,e,f,*]

[a] ISIS Neutron and Muon Facility, Rutherford Appleton Laboratory, Harwell, OX14 0QX, UK

[b] Department of Chemistry, School of Physical and Chemical Sciences, Queen Mary University of London, London, E1 4NS, UK

[c] Cambridge Carbon Capture, UK

[d] Department of Physics, University of Rome Tor Vergata, Piazzale Aldo Moro, 5, 00185via della Ricerca Scientifica 1, 00133 Roma, Italy.

[e] Department of Chemistry, McMaster University, Hamilton, Ontario, L8S 4L8, Canada

[f] Faculty of Land and Food Systems, The University of British Columbia, Vancouver BC, V6T1Z4 Canada

[g] Department of Chemistry and pharmaceutical Sciences, Sapienza University of Rome, Piazzale Aldo Moro, 5, 00185 Roma, Italy.

Authors to whom correspondence should be addressed: kun.tian@uniroma1.it, d.ditommaso@qmul.ac.uk, g.chass@qmul.ac.uk.

Keywords: CO_2, Carbon Utilization, Mineralization, Carbonates, Magnesite, Nesquehonite, Neutron Scattering.

Abstract: CO_2 mineralization via aqueous Mg/Ca/Na-carbonate ($MgCO_3$/$CaCO_3$/Na_2CO_3) formation represents a huge opportunity for the utilization of captured CO_2. However, large-scale mineralization is hindered by slow kinetics due to the highly hydrated character of the cations in aqueous solutions (Mg^{2+} in particular). Reaction conditions can be optimized to accelerate carbonation kinetics, for example, by the inclusion of additives that promote competitive dehydration of Mg^{2+} and subsequent agglomeration, nucleation and crystallization. Towards tracking mineralization and these reaction steps, neutron scattering presents unprecedented advantages over traditional techniques for time-resolved *in situ* measurements. However, a setup providing continuous solution circulation to ensure reactant system homogeneity for industrially relevant CO_2-mineralizsation was currently not available for use on neutron beamlines. We therefore undertook the design, construction, testing and implementation of such a self-contained reactor rig for use on selected neutron beamlines at the RAL-ISIS Neutron and Muon Source (Harwell, UK). The design ensured robust attachment via suspension from the covering flange to stabilize the reactor assembly and all fittings, as well as facilitating precise alignment of the entire reactor and sample (test) cell with respect to beam dimension and direction. The assembly successfully accomplished the principal tasks of providing a continuous flow of the reaction mixture for homogeneity, quantitative control of CO_2 flux into the mixture as well as temperature and pressure regulation throughout the reaction and measurements. The design is discussed, with emphasis placed on the reactor including its geometry, components and all technical specifications. Descriptions of the off-beamline bench tests, safety and functionality, as well as the installation on beamlines and trial experimental procedure are provided, together with representative raw neutron scattering results.

Review of Scientific Instruments
AIP Publishing

I. Introduction

CO_2 mineralization via aqueous Mg/Ca-carbonate ($MgCO_3$/$CaCO_3$) formation represents a huge opportunity for the reuse of captured CO_2,[1] including as a raw material for chemical synthesis (i.e. organic feedstocks and antibiotics),[2] hydrocarbon production (i.e. methane, ethylene and methanol),[3] or in solid materials. Carbonates, which can be used in infrastructure and beyond, have revenues expected to reach $1 trillion/yr. by 2030, according to the Utilization Panel Report: CO_2 Conversion to Solid Carbonates.[1,4-5] Mg^{2+}/Ca^{2+} sources (silicate deposits, wastewater, brine, etc.) are widespread and plentiful and support feasible carbonation on multi gigatonne scales. Available resources of magnesium/calcium including, yet not limited to, silicate-based rocks, are sufficiently abundant to sequester via mineral carbonation, all anthropogenic emissions for the next >1000 years and beyond.[6-7] One example of the mineral carbonation process, for Mg-silicates in this case, embodies the general steps requisite for the process (**Scheme-1**):

$CO_2(g) \rightleftharpoons CO_2(aq)$	**Dissolution**
$CO_2 + H_2O \rightleftharpoons CO_3^{2-} + 2H^+$	**Formation**
$½Mg_2SiO_4 + 2H^+ \rightarrow Mg^{2+} + ½SiO_2 + H_2O$	**Generation**
$Mg^{2+} + CO_3^{2-} \rightarrow MgCO_3(s)$	**Mg-carbonation**

Scheme-1. Chemical steps for conversion of CO_2 gas to Mg-carbonate.

Mg/Ca-carbonation offers the possibility to manufacture CO_2-negative construction materials, which could partially replace ordinary Portland cement (OPC) in certain infrastructure applications.[8] This is crucial because OPC production is responsible for ~8% of man-made CO_2 emissions.[9]

Yet, the synthesis of magnesite (the anhydrous and most valuable form of the Mg-carbonates) at ambient temperature and pressure is notoriously difficult and represents one of the open challenges for the large-scale implementation of CO_2 mineralization.[10-11] This is due to the slow kinetics caused by the highly hydrated character of Mg^{2+} in aqueous solutions ($\Delta G_{hyd}° = -455$ kcal mol^{-1})[12] hindering the initiation of $MgCO_3$ nucleation and subsequent growth. Thus, although $MgCO_3$ is the most stable Mg-carbonate under all conditions and forms slowly in nature at moderate pressures and temperatures,[13] its industrial synthesis is energy-intensive ($120 < T < 185$° C; $P > 100$ bar).[14] Improving the kinetics of $MgCO_3$ precipitation would raise efficacy of its predominance at large-scales in CO_2 mineralization, yet the fundamental aspects are not fully resolved.

Our previous work on the mechanism of Mg^{2+}—H_2O dissociation (i.e. dehydration) established that solution environments and the presence of additives could be highly influential on the processes at

the mineral-water interface as well as on $MgCO_3$ nucleation and growth.[15] Our database of additives promoting Mg^{2+} dehydration and $MgCO_3$ nucleation,[16] has been used in experimental determinations (FTIR, Raman, XRD, SEM/TEM) to evolve our knowledge of the processes controlling aqueous $MgCO_3$ nucleation and growth, with foci on applying this knowledge to accelerate CO_2 mineralization, under industrial conditions with relevant reactant (im)purities. As these traditional characterization techniques are all retrospective in probing the reaction kinetics, to have a real-time nano-scopic 'eye' on these processes would be invaluable. The *in situ* tracking of each crystallization event (dehydration, nucleation, crystal growth), structural changes, dynamical variation and observed kinetics would present a significant evolution in understanding.[17] Such kinetic resolution would help facilitate the rational optimization and acceleration of the carbonation process as well as the nature and properties of the eventual carbonate products.

Neutron scattering offers a means to obtain such information. Neutrons are highly penetrating, (millimeters of aluminium or steel are essentially transparent) which simplifies the reactor design, hence special materials are not requisite for the sample holder window (area where neutron beams pass through). Neutrons are particularly sensitive to hydrogen, so water and hydroxides are easily seen. However, (almost) all elements can be studied by neutrons, so all of the components of the process are accessible. One disadvantage of neutron methods is that they are produced with low beam intensities with respect to other probes, thus requiring sample sizes of typically 1 – 10 g, or more. Yet, in the present case, this is helpful, in that tens of grams of material are present in the reactor. Although this is still small relative to the industrial processes, such multi-gram samples are 'that much closer' to real-world industrial scales (i.e. 3 or 4 orders of magnitude larger than mg amounts) than are conventional laboratory measurements, at the very least hinting at some of the phenomena and challenges that may occur on further scale-up. The time scales in the reaction also suit neutron methods, from the nano- or pico-second dynamics of water to the minutes or hours of the crystallization processes; all well-matched to temporal aspects of neutron scattering.

Hence, the objective was reinforced to develop the technology to track real-time nano- through meso-scopic phenomena driving efficient carbonate growths, with particular focus on magnesite formation. We therefore initiated work to design a prototype CO_2-mineralization reactor for use on selected neutron beamline at the ISIS Neutron and Muon Facility at the STFC Rutherford Appleton Laboratories (RAL-ISIS), in Harwell, UK. It was expected that with such a reactor assembly or 'rig' for *in situ* neutron scattering experiments we would be able to track and to identify reaction conditions (temperature, pCO_2, liquid and gas flow rates, slurry composition, additives) accelerating carbonate

formation and have insights into controlling phase compositions and bulk properties of the output products.

II. Design and production of flow cell reactor rig

A. Original purpose and dimensions

A principal objective was to reproduce the industrial conditions of the mineral-carbonation reactions whilst conducting *in situ* measurements using neutron scattering. This would allow tracking of structural and dynamical changes during the principal CO_2-mineralization steps, including: Mg/Ca-dehydration, aggregation, nucleation and crystal growth. Other measurement techniques could also benefit from the general design of the rig setup (i.e. coherent-THz spectroscopy).[18-19]

Relevant sample environment geometries on these beamlines provided the bases for the overall reactor and component dimensions and design. All activities were actioned with an eye on future comparative hydrogen (H) *vs*. deuterium (D) isotope based experiments (i.e., D_2O and D-labelled Mg-sources such as brucite [$Mg(OD)_2$]), hence the overall reactor volume was constrained to work with 50-100 mL amounts, with D_2O and D-labelled reactants (and costs!) in mind.

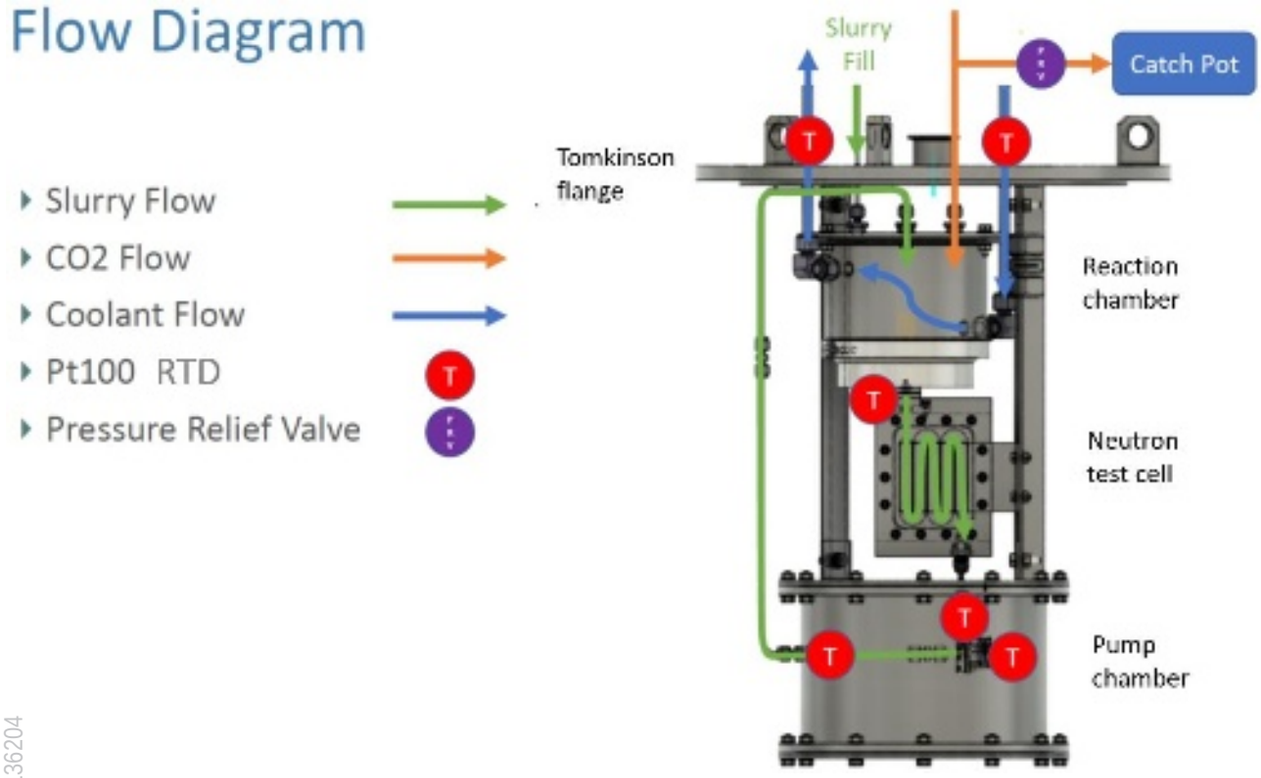

Figure 1. Flow diagram of the reactor rig. Green arrows indicate the flow paths and directions of the reaction slurry; Orange arrows indicate the flow paths and directions of CO_2 gas; blue arrow indicate the flow path and direction of the coolant; T inside red circles are temperature sensors (RTD); PRV inside purple circle is pressure relief valve; Tomkinson flange and the three main components: the reaction chamber, neutron test cell and pump chamber are also indicated.

Structurally, the rig consists of the reaction chamber at the top, neutron test cell in the middle and a 'pump chamber' at the bottom housing a pump to cycle the reactants back up to the reactor and ensure system homogeneity (**Figure.1**). These were built using stainless steel and aluminum alloys, to dampen the contributions to overall weight (and budget!) of the reactor rig. The entire rig assembly is suspended from a 400 mm diameter flange (for historical reasons at ISIS, this is referred to as the Tomkinson flange and rightly-so, thanks John!). The assembly sits in vacuum, to minimize loss of signal caused by air-scattering of neutrons. Each of the three regions of the rig needed to be isolated from the sample environment's vacuum tank for obvious reasons including avoiding reactants being siphoned off and out of the reactor and into the sample chamber, else from the pump whose seals and gaskets have manufactured tolerances to external pressures/vacuums, yet not to the degree of the sample environs (1×10^{-6} bar, or lower). Externally, the reactor design allowed for the introduction of reactants and CO_2 gas into the reaction chamber from outside the sample area, above the Tomkinson flange.

The neutron test cell was designed with a serpentine shape to ensure sample homogeneity when in the beam (**Figure.2**); helping to avoid 'cornering' with some sample being stuck in the corners and

not efficiently reacting, whilst reducing overall reaction homogeneity, potentially and progressively skewing relevance of the scattering measurements relative to the overall reaction mixture.

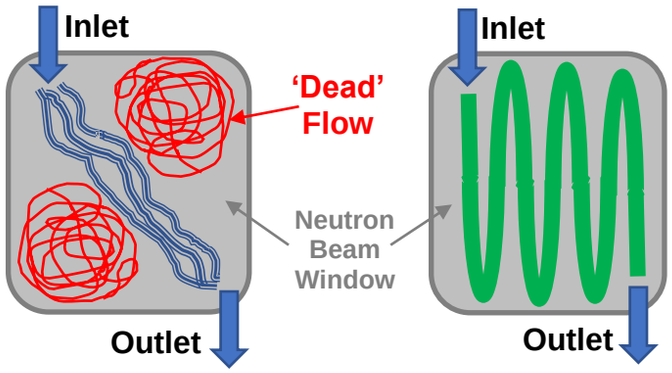

Figure 2. Schematic of the sample cell, with graphical illustration of the importance of directed (serpentine) flow to ensure the reaction mixture is homogeneous across the neutron beam during measurements. (*Left*) in the absence of a channel, areas of 'dead flow' arise and are not cycled to the reaction chamber to react with incoming CO_2 gas or additives.

With respect to measurements to be undertaken, at the outset static measurements were planned for all reactants, additives and solvents to acquire base values for these systems at ambient temperature and pressure, the ideals for industry. Preliminary runs of these 'static' systems were conducted away from the neutron beamlines to ensure safety and functionality of the rig. The subsequent on-beamline, 'live' runs of these static systems allowed for any issues arising to be identified prior to the longer mineralization reaction measurements, which were conducted over 24-48 hours.

Tracking of the mineralization reactions were accomplished through initial measurements on slurries of unreacted Mg-sources (i.e. brucite) followed by the introduction of CO_2 to initiate the mineralization reaction, again, under industrially ideal conditions, maintained over the course of the entire mineralization reaction process (~24-48 hrs).

B. Design

The entire reactor rig and all fasteners were constructed with a mix of aluminum and A2/304 stainless steel throughout; with thermal control of up to a maximum of 100 °C. A priority requirement was that the rig had to be a closed system in order to isolate the reaction components and products from the vacuum of the sample environment on the neutron beamlines. Within this closed system, the reactor provided an environment where the Mg-rich aqueous slurry (Mg-hydroxide in the first instance) could react with the CO_2 gas being introduced into the rig from an external source, above the Tomkinson flange. The reactor inlet nebulized the slurry from above via a spray nozzle, with the objective of attaining high surface-area:volume ratios of the droplets to raise reactivity with CO_2 and homogeneity of the product. The positive displacement pump in the bottom pump chamber ensured

flow, with the reacting slurry being pulled down to the bottom of the reaction chamber and into the neutron test cell, then pumped back to the top and back into the reactor via the nebulizer nozzle.

Details of all components of the rig from top to bottom (**Figure. 1**) follow:

1. Reaction chamber: Consists of a 304/304L stainless steel double walled cylindrical vessel of 500 mL total, with a ~50-500 mL working volume. The inner volume is used for the CO_2 mineralization reaction up to a maximum of 3 bar absolute working pressure. The annular gap is a cooling jacket designed to hold glycol-based coolant (driven from a Julabo FP5x series water bath), used to control the temperature of the reaction and is rated to 2 bar absolute working pressure. The layout of the reaction chamber can be seen in **Figures. 1** and **3A**; more detailed engineering blueprints are presented in **Figures S1-1** to **S1-6**.

2. Neutron test cell: Consists of a 6082-T6 aluminum rectangular flat cell. It is a two-piece construction that hosts an interior 70×70×1 mm serpentine-grooved space to guide the flow (**Figures.2**, **3B1**-**B2**, and **S2-1**, **S2-2**). It is rated to 3 bar absolute working pressure.

3. Pump chamber: Consists of a 304/304L stainless steel single walled vessel. The chamber (**Figures. 3C1**-**C2** and **S3-1** to **S3-4**) houses the positive displacement pump (TCS Micropumps R400BL conical revolution pump, TCS Micropumps Ltd., Faversham, UK) and is vented to the atmosphere via a ~2.5cm (1") tube through the Tomkinson flange; the pump's wiring is taken out through the venting tube (**Figures. 4** and **S4**). The principal purpose of the bottom pump chamber was to isolate the positive displacement pump from the sample environment and its ultra-low-pressure (quasi-vacuum). Within the bottom chamber, the ambient air around the pump helped to maintain temperature within operating temperatures of the pump.

The entire reactor rig was secured with bolts underneath the Tomkinson flange (**Figure. S4**). The flange is made from 304/304L stainless steel and has the following components welded on: 3-off fixed lifting points, 2-off KF40 flanges, 2-off 6 mm reaction chamber inlet/outlet tubes, 2-off 1/2" reaction chamber coolant jacket inlet/outlet tubes and 2-off brackets.

C. Manufacture and assembly

The components were manufactured by Genesis Precision and ABC Stainless Steel, which were then subsequently assembled in-house.

D. Testing

1. Bench testing

Bench tests of the rig were conducted to optimize the reaction chamber spray nozzle design and also to establish the maximum viscosity slurry concentration that could homogeneously flow through the system. Both the reaction chamber and neutron test cell were covered with clear plastic covers for this testing to provide capabilities for visual tracking (**Figure. S5**).

2. Pressure Testing

All components in the reactor rig assemble were proof tested at ambient pressure and above to ensure performance under pressure variance, as follows: the reaction chamber was tested at 5.6 barA (pump chamber) and at 3 barA (annular gap) and the test cell was tested at 5.6 barA, with each successfully supporting these higher pressures.

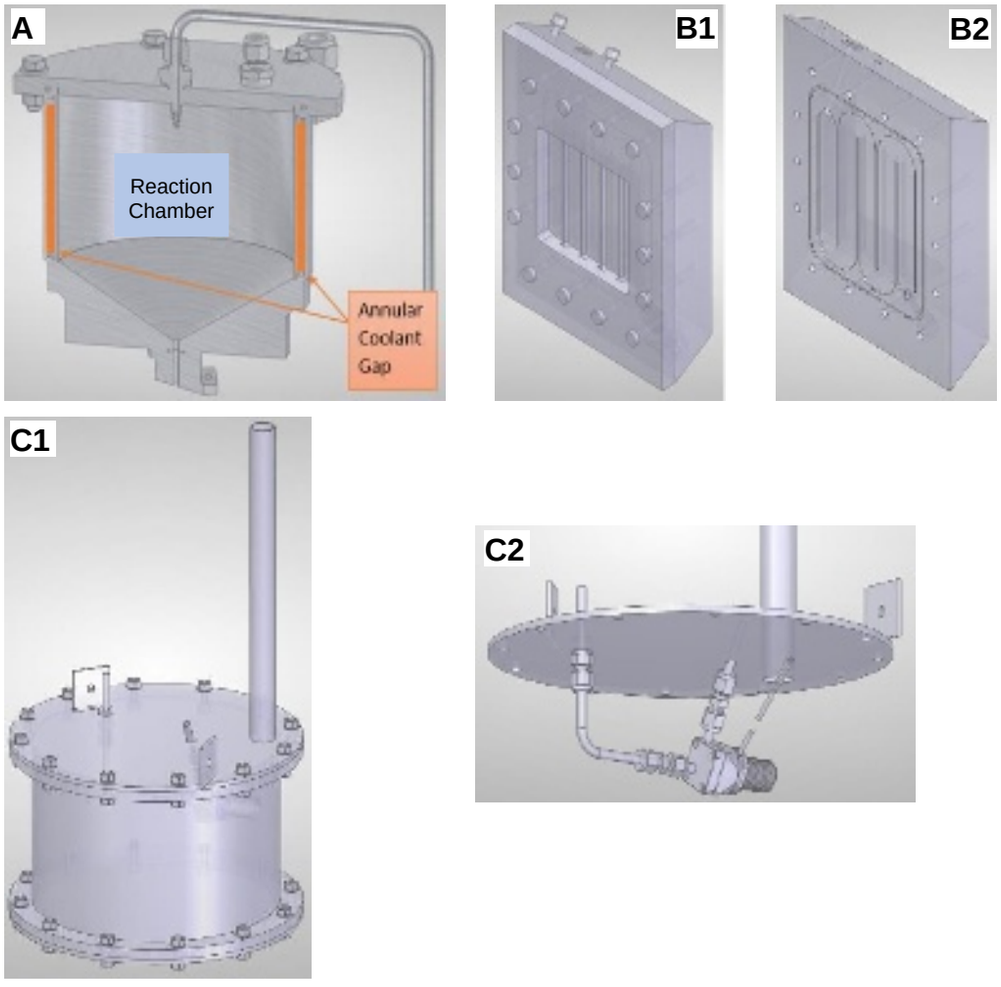

Figure 3 The three principal components of the CO_2-mineralization reactor rig are as follows: (A) reaction chamber; (B) neutron test cell, with (B1) covering cap on and (B2) open, showing serpentine flow path; (C) pump chamber, with views (C1) from outside, with chamber closed and (C2) inside, with pump and flow lines.

3. Leak Testing

The system was vacuum and leak tested by the RAL-ISIS Pressure and Furnace division prior to being placed on any beamlines. Joints were tightened until acceptable sustained seals at 2×10^{-8} mbar.l.s^{-1} were attained.

III. Experiments and exemplary data

A. Rig placement in beamline and assemblage

For placement and use of the reactor rig assembly on neutron beamlines at RAL-ISIS, the following operational procedure was actioned:

The rig was initially physically fixed to hang underneath a standard Tomkinson flange through securing onto a 3 metal-pole frame which was then secured to the flange. This was then lowered with a crane into the vacuum tank that the rig was designed to fit; in this case IRIS/OSIRIS beamline. The neutron test cell was aligned to be perpendicular to the direction of the neutron beam and the flange-reactor assembly fixed in place (**Figure. 4**).

An external CO_2 gas cylinder was then connected to the reactor assembly via a valve and mass flow controller fitted to the top of the Tomkinson flange including the following: slurry inlet, CO_2 inlet and pressure release valve (PRV), coolant inlet/outlet and a thermocouple (**Figure. 1**). The vacuum pump was used to remove all the air from the reaction chamber. The pressure stabilized at -98 kPa due to vaporization of the water in the chamber. The valve was then closed and the pressure gauge monitored for about a minute. If pressure creeps back up, it is indicative of a leak. The pressure in the sample chamber was monitored till it stabilizes at approximately -99 KPa; any varied readings signaling leakage from the reactor rig assembly.

Figure 4 The CO_2-mineralization reactor rig being installed into the sample area of the IRIS beamline at RAL-ISIS. The rig position is adjusted such that the neutron test cell is perpendicular to the incident neutron beam (N)

B. Sample preparation and loading

An aqueous brucite [$Mg(OH)_2$] slurry was made by adding 29.16 g brucite (99.3%, Luvomag H002, Lehmann&Voss&Co., Hamburg, DE) to 500 mL of deionized water. This amount was added despite brucite's sparingly solubility in water to provide abundance of Mg, with the water serving as mobile phase to assist in moving the thick slurry and dissolution of CO_2. The continual use of Mg to form Mg-carbonates aiding with the perennial battle against the low solubility of brucite. A large syringe was used to transfer the slurry into the reactor, injecting into the nebulizer assembly installed into the top lid of the reaction chamber. The -50 KPa vacuum from the positive displacement pump in the bottom 'pump chamber' of the assembly assists with this and getting the reaction mixture flowing through the rig.

C. Reaction commencement and neutron data acquisation

The initiation of measurements involved opening the neutron beam shutter and adjusting to ~90% transmission to help reduce the amount of multiple scattering, as with other metal-containing samples, systems and setups.[20,21] The CO_2 reactant gas was introduced by opening the gas cylinder valve and adjusting the regulator to a flux of 5-17 standard cubic centimeters per minute (SCCM) using a mass

flow controller (MFC) (HFM-300 flow meter, equipped with HFC-302 flow controller and THCD-100 configurable display, Teledyne Hastings Instruments, Hampton, USA) for the incoming CO_2 gas, to keep reaction at a steady rate. Throughout the ensuing mineralization reaction, the pressure and the MFC were monitored continuously.

Once the reaction was complete, measurements were ceased and the neutron beam shutter closed, terminating irradiation of the reactor rig and initiating the cool-down phase. This involved lifting the rig assembly out of the sample area on the beamline and placing it in a radiation shielded environs (steel cylinder) to allow the induced activity to decay to a safe level (typically ~7-10 days). It was then possible to open the reactor to remove the output Mg-carbonate products (**Figure. 5 left**) and subsequently analyze relevant properties of the reactant mixture (now a mix of product and unreacted starting components), including: identity, structure and purity with X-ray diffraction (XRD) and other spectroscopic techniques (FTIR, Raman, coherent-THz) as well as imaging with electron microscopy (SEM, TEM). The XRD spectrum of the reaction product being in close resemblance with that of nesquehonite proved $MgCO_3$ hydrate was produced during the full scale test of the rig (**Figure. 5 right**).

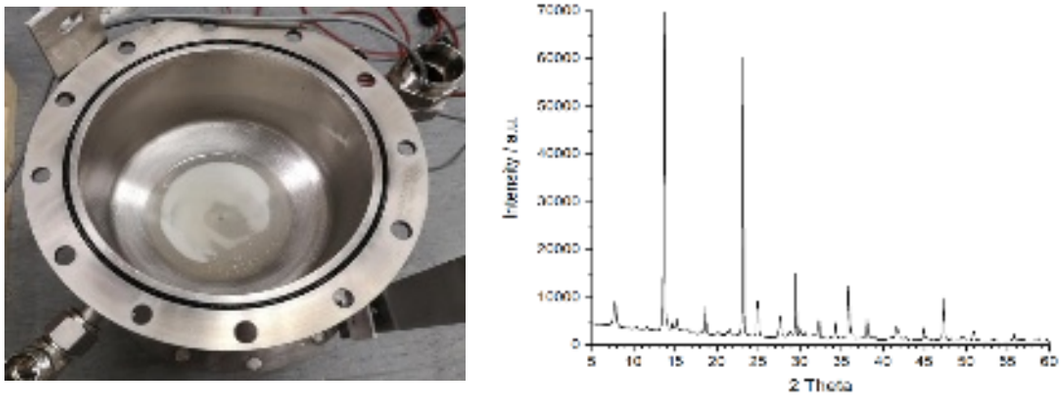

Figure 5 (*Left*) The open reaction chamber (top view) with residual product carbonates; the remainder being in the neutron test cell and piping throughout the reactor, subsequently flushed for recovery. (*Right*) XRD spectrum of the reaction product, in close resemblance with that of nesquehonite.

D. Exemplar spectrum and reaction product

Representative QENS spectra at a Q vector of Q=0.6 ± 0.2 $Å^{-1}$ as a function of time, acquired on the IRIS beamline at RAL-ISIS, are presented in **Figure. 6**. Included in the figure is the contribution of the empty rig, which is negligible to the measured signal. The large quasielastic broadening of the spectra (spectrometer resolution FWHM = 0.018 meV) is a signature of stochastic motions of the dominant scattering component, the hydrogen atoms. That broadening is reasoned by translational and rotational motions of the hydrogen atoms. The amplitude of the QENS signal is sensitive to changes in the mobility of hydrogen atoms in the sample. The slower the particles move, the sharper the line shape becomes and the quasielastic amplitude at zero energy transfer increases. After the reaction with CO_2 started at t=0 each 30 min a spectrum was recorded. In **figure 6** on the left side the evolution of some spectra with time is shown, which clearly demonstrates that the quasielastic scattering amplitude is increasing with reaction time. From the observed increase of the amplitude in **Figure. 6** we can conclude that the stochastic motions are slowing down, which indicates that larger molecular complexes are growing in solution over time and the CO_2-mineralization reaction can thus be followed in time. The amplitudes of these spectra were then integrated around zero energy transfer with the energy resolution of the spectrometer as integration limits. In **Figure. 6** (right) the integrated amplitude at zero energy transfer is shown over all the recorded spectra against the reaction time. It clearly demonstrates that the quasielastic amplitude can follow the reaction process over time. The observed changes are far bigger than the error bars. After about 15 hours the amplitude saturates and signals the end of the reaction. A more detailed discussion about the changes in the lineshape and their relation to reaction products will be given in a forthcoming publication.

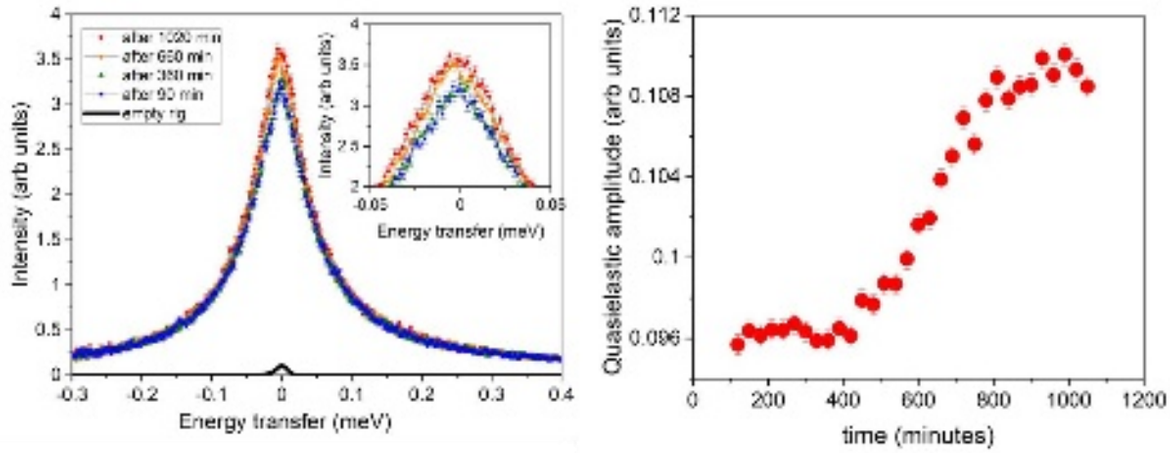

Figure 6 (*Left*) *Time-resolved QENS spectra acquired on the IRIS beamline at Q= 0.6 Å^{-1}. Inset: zoom in of the central peaks. (Right) The time-resolved integrated quasielastic peak amplitude from all recorded spectra on the left side as a function of reaction time.*

IV. Discussion

A. Functionality

The 3 cm × 2 cm beam size determines the minimum cross-sectional area of the neutron test cell, for achieving highest signal. To achieve a beam transmission of ~90% (to minimize multiple scattering), a neutron test cell thickness of ~1 mm was requisite. Due to this size limitation, the serpentine design was deemed optimal for maximizing surface area, flow path, continuous flow and homogeneity. However, this did raise concerns regarding the hardening and/or sticking of the reaction mixture in the serpentine 'S' curves of the neutron test cell as well as presenting a challenge to flow through the 1 mm diameter tubing and the pump in the bottom pump chamber. Encouragingly, during initial and subsequent test-runs there were no issues arising regarding either the pipe diameter or the hardening of the slurry.

A nebulizer (impingement pin spray nozzle) was installed in the inlet to the reactor for sparging the reaction mixture and create a fine spray of brucite slurry to maximize the surface area of slurry exposed to the carbon dioxide, also assisting in raising homogeneity of the mixture.

B. Shortcomings and lessons learnt

Overall, the rig is awkward to assemble, disassemble, clean and use. With more time for development and construction, the design could have been refined further. Further, the supporting posts holding the reactor assembly together and allowing attachment to the Tomkinson flange, presented 'blind

spots' for the neutron beams, especially on IRIS with its wide range of detector angles. Scattering data at these angles are missing, and lowered the signal-to-background ratio.

The rig is also heavy and unwieldy, partly because the Tomkinson flange is made from stainless steel. Using aluminum would have made the rig lighter, but more expensive and harder to weld. It would also have required feedthroughs for the stainless steel tubing, instead of directly welding them to the flange.

The "cooling off" procedure after each use means that the rig is effectively single use on a short-term scale (one use every ~1-2 weeks at best). A possible solution would be to have storage tanks and diverting valves for emptying the reactor whilst on the beamline, which could then be flushed and readied for the next reactions.

C. Future improvements and work

This rig, or a similar design could be used to study other low solubility substance reaction and formation.

A 2nd-generation reactor rig with a storage tank will be designed and manufactured for future experiments.

V. Summary

Herein, we present the design, development and initial sample runs of a self-contained flow cell reactor rig assembly for *in situ* neutron scattering measurements of aqueous CO_2 mineralization with industrially representative reactants and under industrial conditions. The overall performance of the rig is satisfactory and has enabled us to acquire for the first time high-quality time-resolved neutron spectra of CO_2 mineralization to Mg-carbonates. The rig has been used on two different beam lines at ISIS and could be used on several others; modular design would allow even wider use, for example on any beamlines anywhere. Several lessons have been learned on how to resolve shortcomings and to optimize future design, especially for use on differing beamline sample environments, as well as for completing multiple reactor runs on differing reactant systems without having to remove the rig from the beamline and waiting for the induced activity to decay, in order to reuse the reactor.

SUPPLEMENTARY MATERIAL

See supplementary material for the detailed design diagrams and schemetics of each component of the reactor rig.

ACKNOWLEDGEMENTS

The authors acknowledge STFC's Impact Acceleration Account funding (PRNZZD9R, 2020), EU-Horizon 2020 and BEIS, UK for supporting the FUNMIN project (ACT, No. 299668) and providing the means to extending ongoing work to cementitious materials. The STFC RAL is thanked for access to neutron beam facilities via the following proposals related to the evolution of this work to making requisite the construction of this rig: RB1710285, RB1710444, RB1710447, RB2010426 and RB2010696. Modern Age Plastics Inc., Toronto, Canada is thanked for supporting the development of related carbonate reactors helping to inform on this work and *vice versa*.

AUTHOR DECLARATIONS

Conflict of interest

The authors have no conflicts to disclose.

Author Contributions

AM & MD: Investigation (supporting). **FS:** Investigation (equal). **ME:** Methodology (equal); Investigation (supporting). **RC:** Methodology (equal); Investigation (lead); Writing – review & editing (equal). **GR & FD:** Investigation (equal); Writing – review & editing (equal). **DHF:** Resources (lead); Writing – review & editing (equal). **SFP:** Methodology (equal); Writing – review & editing (equal). **KVT:** Validation (lead); Writing – Original draft (lead); Writing – review & editing (equal). **DDT:** Funding acquisition (lead); Project administration (equal); Writing – review & editing (equal). **GAC:** Conceptualization (lead); Funding acquisition (equal); Project administration (equal); Methodology (lead); Investigation (lead); Supervision (lead); Validation (lead); Writing – review & editing (lead).

DATA AVAILABILITY

The data that support the findings of this study are available from the corresponding author upon reasonable request.

REFERENCES

[1] Mission Innovation, Accelerating Breakthrough Innovation in Carbon Capture, Utilization, and Storage, Houston, Texas, 2017.
[2] W. H. Mu, G. A. Chass, D. C. Fang. J. Phys. Chem. A, 112, 6708 (2008).
[3] CG. Centi and S.Perathoner. Catalysis Today, 148, 191 (2009).
[4] The Growing Role of Minerals and Metals for a Low Carbon Future, World Bank Group (2017). Available at: http://hdl.handle.net/10986/28312
[5] M. S. Imbabi, C.Carrigan, and S, McKenna, Int. J. Sustain. Built Environ. 1, 194 (2012).
[6] A. Sanna, M. Uibu, G. Caramanna, R. Kuusik, and M. M. Maroto-Valer, Chem. Soc. Rev. 43, 8049 (2014).
[7] K. S. Lackner, Annu. Rev. Energy Environ. 27, 193 (2002).
[8] S. Mignardi, C. De Vito, V. Ferrini, R. F. Martin, J. Hazard. Mater. 191, 49 (2011).
[9] K. L. Scrivener, V. M. John, and E. M. Gartner, Cem. Concr. Res. 114, 2 (2018).
[10] A. M. Gaines, Science 183, 518 (1974).
[11] R. S. Arvidson and F. D. Mackenzie, Am. J. Sci. 299, 257(1999).
[12] D. Di Tommaso and N. H. de Leeuw, J. Phys. Chem. B 112, 6965 (2008).
[13] M. Hänchen, V. Prigiobbe, R. Baciocchi, and M. Mazzotti, Chem. Eng. Sci. 63, 1012 (2008).
[14] E. J. Swanson, K. J. Fricker, M. Sun and A-H. A. Park, Phys. Chem. Chem. Phys. 16, 23440 (2014).
[15] D. Toroz, F. Song, G. A. Chass, and D. Di Tommaso, CrystEngComm. 23**,** 4896 (2021).
[16] D. Toroz, F. Song, A. Uddin, G. A. Chass, and D. Di Tommaso, Cryst. Growth Des. 22**,** 3080 (2022).
[17] K. V. Tian, M. Z. Mahmoud, P. Cozza, S. Licoccia, D.-C. Fang, D. Di Tommaso, G. A. Chass, and G. N. Greaves, J. Non-Cryst. Solids 451**,** 138 (2016).
[18] K. V. Tian, B. Yang, Y. Yue, D. T. Bowron, J. Mayers, R. S. Donnan, C. Dobó-Nagy, J. W. Nicholson, D.-C. Fang, A. L. Greer, G. A. Chass and G. N. Greaves, Nat. Commun. 6**,** 8631 (2015).
[19] F. V. Song, B. Yang, D. Di Tommaso, R. S. Donnan, G. A. Chass, R. Y. Yada, D. H. Farrar, and K. V. Tian, Mater. Adv. 3**,** 4982 (2022).
[20] K. V. Tian, G. Festa, F. Basoli, G. Laganà, A. Scherillo, C. Andreani, P. Bollero, S. Licoccia, R. Senesi, and P. Cozza, Dent. Mater. J. 36, 282 (2017).
[21] K. V. Tian, F. Passaretti, A. Nespoli, E. Placidi, R. Condò, C. Andreani, S. Licoccia, G. A. Chass, R. Senesi, and P. Cozza, Nanomaterials 9, 1119 (2019).

Flow Diagram

- Slurry Flow
- CO2 Flow
- Coolant Flow
- Pt100 RTD
- Pressure Relief Valve

AIP Publishing

Review of Scientific Instruments

ACCEPTED MANUSCRIPT

PLEASE CITE THIS ARTICLE AS DOI: 10.1063/5.0136204

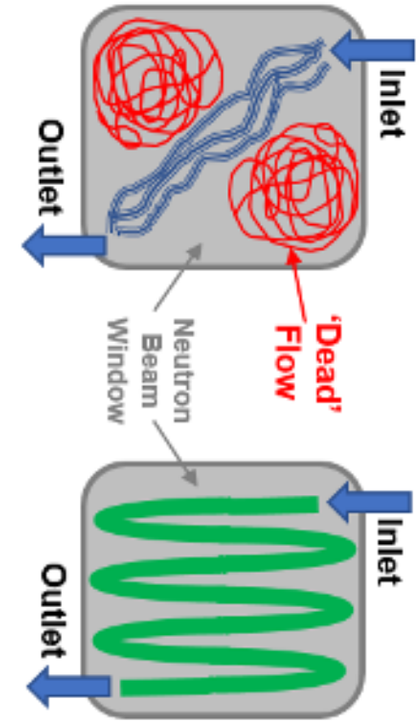

AIP Publishing

Review of Scientific Instruments

ACCEPTED MANUSCRIPT

PLEASE CITE THIS ARTICLE AS DOI: 10.1063/5.0136204

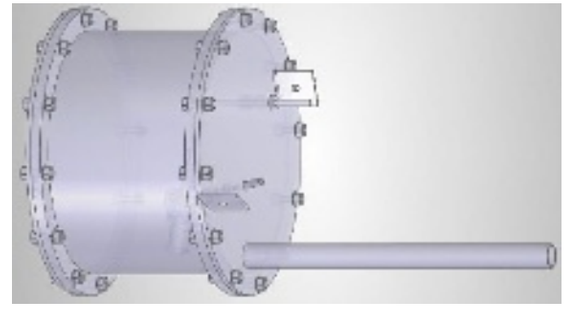

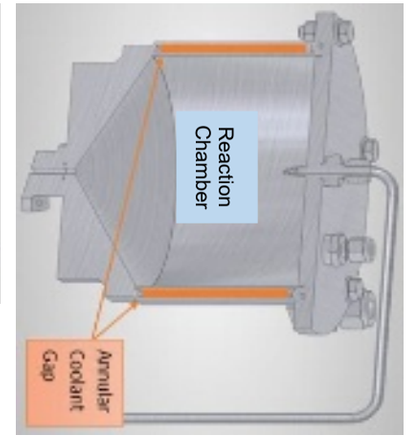

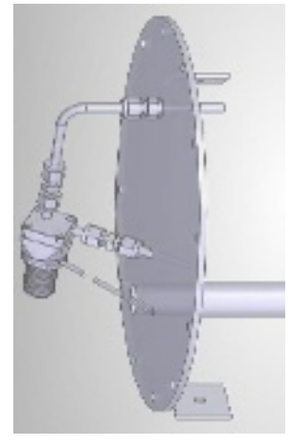

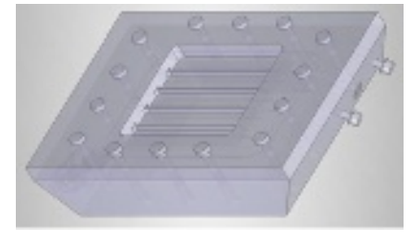

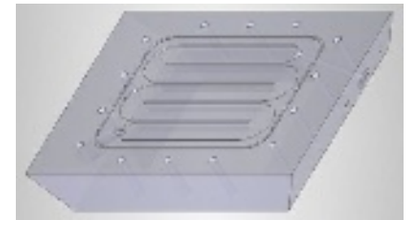

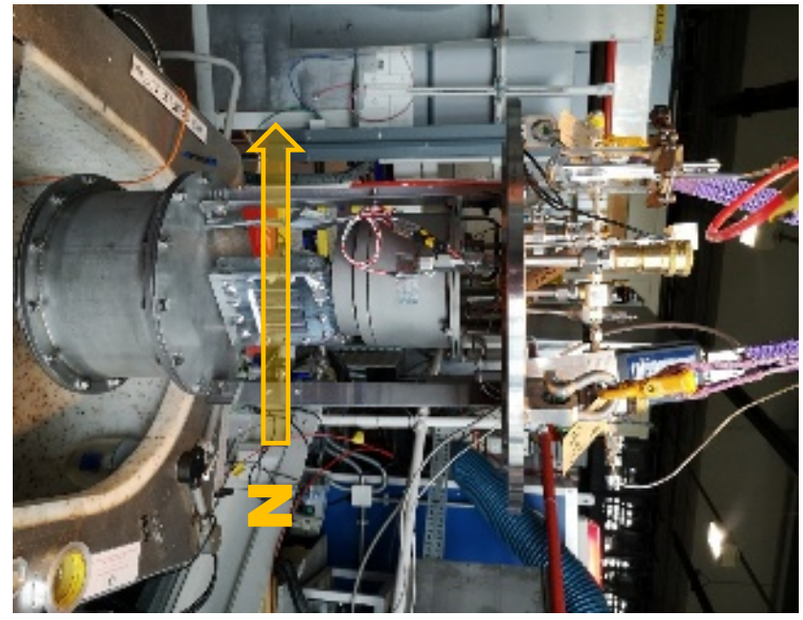

AIP Publishing

Review of Scientific Instruments

ACCEPTED MANUSCRIPT

This is the author's peer reviewed, accepted manuscript. However, the online version of record will be different from this version once it has been copyedited and typeset.
PLEASE CITE THIS ARTICLE AS DOI: 10.1063/5.0136204

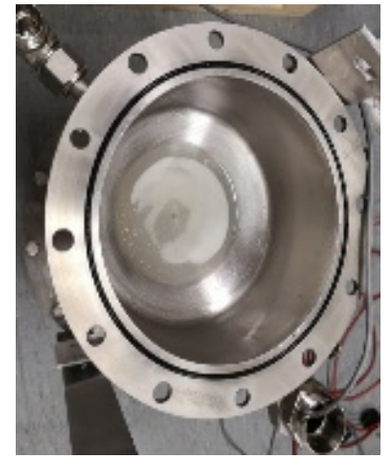

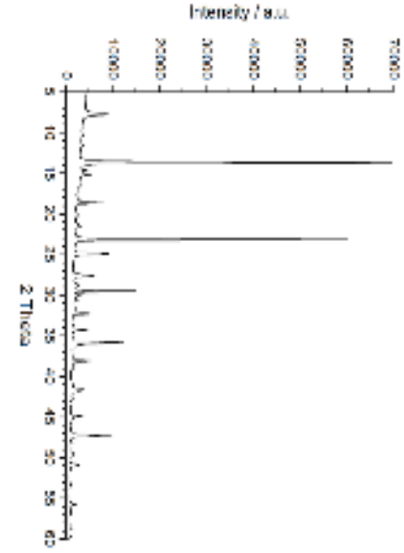

AIP Publishing

Review of Scientific Instruments

ACCEPTED MANUSCRIPT

This is the author's peer reviewed, accepted manuscript. However, the online version of record will be different from this version once it has been copyedited and typeset.
PLEASE CITE THIS ARTICLE AS DOI: 10.1063/5.0136204

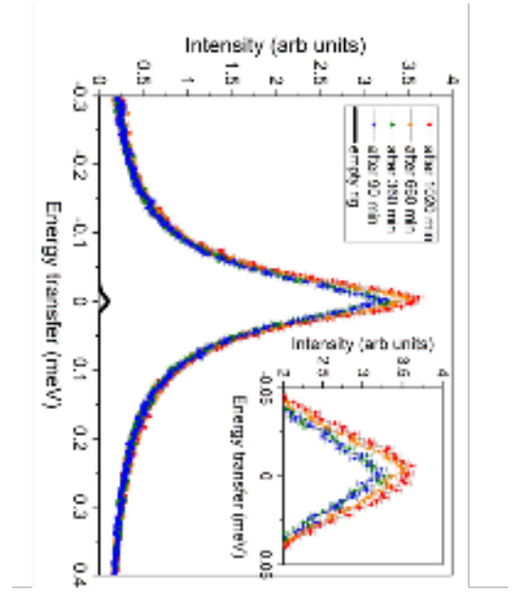

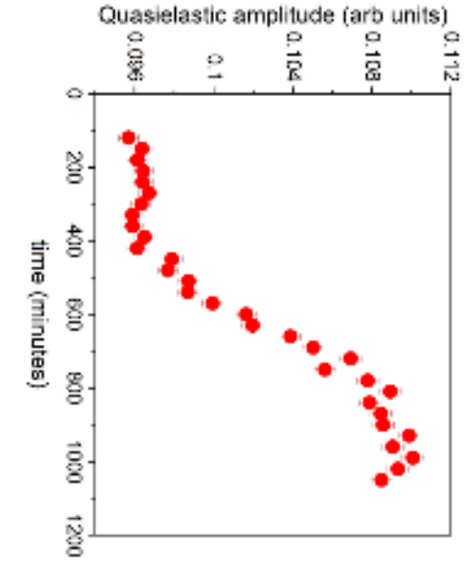

$\mathbf{CO_2(g)} \rightleftharpoons CO_2(aq)$	**Dissolution**
$CO_2 + H_2O \rightleftharpoons CO_3^{2-} + 2H^+$	**Formation**
$½Mg_2SiO_4 + 2H^+ \rightarrow Mg^{2+} + ½SiO_2 + H_2O$	**Generation**
$\mathbf{Mg^{2+} + CO_3^{2-} \rightarrow MgCO_3(s)}$	**Mg-carbonation**